Stationary light pulses in cold thermal atomic clouds

Jin-Hui Wu,[1,*] M. Artoni,[2,3] and G. C. La Rocca[4]
[1]*College of Physics, Jilin University, Changchun 130023, P.R. China*
[2]*Department of Physics and Chemistry of Materials CNR-IDASC Sensor Laboratory, Brescia University, Brescia, Italy*
[3]*European Laboratory for Nonlinear Spectroscopy, Firenze, Italy*
[4]*Scuola Normale Superiore and CNISM, Pisa, Italy*
(Received 13 March 2010; published 12 July 2010)

Fourier-expanded Maxwell-Liouville equations are employed to study the light pulse dynamics in atomic samples coherently driven by a standing-wave light field. Solutions are obtained by a suitable truncation of the Maxwell-Liouville equations that contain the number of spin and optical Fourier coherence components appropriate to the sample temperature. This approach is examined here for cold but thermal atoms where the Doppler broadening is still not negligible and familiar secular approximations no longer hold. In this temperature regime higher-order momentum Fourier coherence components are shown to be important for achieving excellent agreement with a recent experiment done in cold ^{87}Rb clouds at several hundred microkelvins.

DOI: 10.1103/PhysRevA.82.013807 PACS number(s): 42.50.Gy, 42.70.Qs, 42.50.Hz

I. INTRODUCTION

The development of quantum memories for photonic states [1–3] hinges on the controlled localization and storage of weak light pulses. Apart from the fundamental interest, schemes for manipulating the propagation dynamics of weak light pulses are being pursued rather actively for practical implementations [4,5]. Such schemes have already led to novel approaches for reversible light storage and retrieval [6–9], adiabatic population and coherence transfer [10–12], and resonant enhancement of optical nonlinearities [13–16], just to mention a few. Most of these studies deal with spatially homogeneous atomic samples driven by external *traveling-wave* (TW) light beams, which significantly modify absorption and dispersion properties of the dressed samples through electromagnetically induced transparency (EIT) [17–19]. Schemes with atomic samples driven into a regime of *standing-wave* (SW) EIT have also been well studied [20–24]. As far as the electromagnetic confinement is concerned, SW-EIT driving schemes represent a real improvement and may in fact be exploited either to realize all-optically tunable photonic bandgap structures [25–28] or to generate stationary light pulses (SLPs) [29–36] whose forward (FW) and backward (BW) components can easily be stored, made to interact, or read out of the sample. This versatility in the control over the propagation of SLP components may ease the realization of nonlinear interactions between weak light pulses [37–40] where strong atom-photon couplings are required for quantum information processing [41–44].

Driving atomic systems in a SW-EIT configuration, however, is not a straightforward extension of the TW-EIT configuration [42,45]. In an SW driving configuration, higher-order momentum components of spin and optical coherences are expected to arise due to multiple coherent scattering of the FW and BW components of a probe field off the SW optical grating. These higher-order components are actually responsible for significant loss and diffusion in the decay process of SLPs in ultracold atomic samples [46], where they indeed preserve their coherence [31,42,45]. Conversely, these higher-order components are not important in warm atomic samples, where instead they quickly decohere due to the fast atomic motion [30,31].

Although different approaches to studying the propagation dynamics of weak light pulses in the presence of SW optical gratings have been developed for ultracold atomic samples with negligible Doppler broadening [31,42,46] and for warm atomic samples through a secular approximation [29,30], yet a complete description at low but finite temperatures is still missing. At these temperatures the Doppler broadening and higher-order coherence components are important and need to be taken into account. SLP dynamics in cold but thermal atoms has been observed in a recent experiment [32] whose results are interpreted[1] by resorting to spin coherences of order ± 2 besides the zero-order spin coherence and optical coherences of order ± 1.

The purpose of the present article is to extend the approach we developed in Ref. [46] to the low but finite temperature regime, with proper inclusion of the Doppler effect arising from the atomic random motion. Our approach, strongly supported by recent experimental work carried out in SW dressed cold thermal ($T \sim$ mK) ^{87}Rb atoms [32], is easily reduced to study the light pulse dynamics in ultracold ($T \sim \mu$K) and warm ($T \sim 300$ K) atoms driven by an SW coupling field. We proceed by giving in Sec. II the appropriate infinite set of Maxwell-Liouville equations whose solutions are spatially periodic atomic coherence components which now depend on the atomic velocity and have been integrated over a typical velocity distribution [47,48]. The general approach developed in Sec. II is then employed in Sec. III to reproduce well the experimental data on cold thermal ^{87}Rb atoms in Ref. [32]. In particular, we show a substantial

*jhwu@jlu.edu.cn

[1]Neither the Doppler broadening nor fairly higher-order coherence components are directly included in Ref. [32], which is somehow overcome by adopting rather high dephasing rates for the spin coherence components of order ± 2. Note that this fails, in the end, to recover the fine structure of the observed data. See, e.g., the relevant discussion of Fig. 4.

departure from the experiment when we purposely neglect the residual Doppler broadening. Moreover, solving the Maxwell-Liouville equations in Sec. II entails a suitable truncation procedure where only a few relevant higher-order components of spin and optical coherences are included, without altogether discarding higher-order coherence components as typically done through a secular approximation [29,30]. This truncation clearly depends on the atomic temperature through the Doppler broadening. In addition, a bichromatic SW driving configuration is expected to quench the onset of higher-order coherence components [45] in much the same way that the Doppler effect does. This has actually been used in Ref. [32] to create a two-color SLP. The bichromatic SW driving configuration has also been included in the model in Sec. II and used in Sec. III to recover numerically the relevant experimental results observed in Ref. [32].

II. THEORETICAL MODEL AND BASIC EQUATIONS

We consider here a three-level atomic system with two lower levels, $|1\rangle$ and $|2\rangle$, and one excited level $|3\rangle$ (see Fig. 1), which may represent, for example, the hyperfine states $|5S_{1/2},F=1\rangle$, $|5S_{1/2},F=2\rangle$, and $|5P_{3/2},F'=2\rangle$ of ^{87}Rb atoms, just as done in Ref. [32]. The transition $|2\rangle \leftrightarrow |3\rangle$ is driven by a bichromatic SW *coupling* electric field with one (FW) component of frequency $\omega_{c_+}=ck_{c_+}$ traveling in the $+z$ direction and another (BW) component of frequency $\omega_{c_-}=ck_{c_-}$ traveling in the opposite $-z$ direction, which is described by

$$E_c = E_{c+}e^{-i\omega_{c+}t+ik_{c+}z} + E_{c-}e^{-i\omega_{c-}t-ik_{c-}z}. \tag{1}$$

In the presence of an incident (FW) weak probe of frequency $\omega_{p_+}=ck_{p_+}$ that couples to the transition $|1\rangle \leftrightarrow |3\rangle$, a similar probe of frequency $\omega_{p_-}=ck_{p_-}$ and scattered in the opposite (BW) direction will also be generated through wave mixing with the bichromatic coupling field, and the *probe* field can then be written as

$$E_p = E_{p+}e^{-i\omega_{p+}t+ik_{p+}z} + E_{p-}e^{-i\omega_{p-}t-ik_{p-}z}. \tag{2}$$

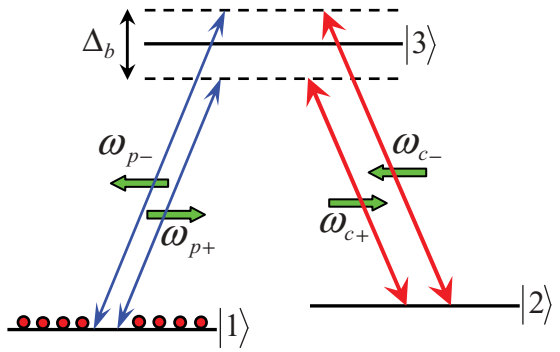

FIG. 1. (Color online) Energy level diagram for atoms in a typical *bichromatic* standing-wave driving configuration [32,45]. When the FW (ω_{c+}) and BW (ω_{c-}) coupling beams are slightly detuned, by $\Delta_b=\omega_{c-}-\omega_{c+}$, an incident FW probe ($\omega_{p+}$) leads to the formation of a BW (ω_{p-}) probe with the same frequency detuning Δ_b. The detuning choice shown here corresponds to a specific case discussed in Sec. III, whereas the limit case $\Delta_b=0$ corresponds to the usual *monochromatic* standing-wave driving configuration [29–31].

In particular, an FW probe photon (k_{p_+}) and a BW coupling photon (k_{c_-}) may coherently scatter into an FW coupling photon (k_{c_+}) and a BW probe photon (k_{p_-}) so as to conserve momentum ($k_{p_+}+k_{c_-}=k_{p_-}+k_{c_+}$) and energy ($\omega_{p+}+\omega_{c-}=\omega_{p-}+\omega_{c+}$).

In the usual electric-dipole and rotating-wave approximations the interaction Hamiltonian is [17,39]

$$H_I(z,t) = -\hbar\Omega_p(z,t)\,|3\rangle\langle 1| - \hbar\Omega_c(z,t)\,|3\rangle\langle 2| + \text{H.c.}, \tag{3}$$

where the probe and coupling Rabi frequencies can be written as

$$\begin{aligned}\Omega_p(z,t) &= \Omega_{p+}(z,t)e^{-i\Delta_{p+}t+ik_{c+}z} + \Omega_{p-}(z,t)e^{-i\Delta_{p-}t-ik_{c-}z}\\ &= [\Omega_{p+}(z,t)+\Omega_{p-}(z,t)e^{-i\Delta_b t-i(k_{c+}+k_{c-})z}]\\ &\quad\times e^{-i\Delta_{p+}t+ik_{c+}z},\\ \Omega_c(z,t) &= \Omega_{c+}(t)e^{-i\Delta_{c+}t+ik_{c+}z} + \Omega_{c-}(t)e^{-i\Delta_{c-}t-ik_{c-}z}\\ &= \left[\Omega_{c+}(t)+\Omega_{c-}(t)e^{-i\Delta_b t-i(k_{c+}+k_{c-})z}\right]e^{-i\Delta_{c+}t+ik_{c+}z},\end{aligned} \tag{4}$$

Here $\Delta_{p\pm}=\omega_{p\pm}-\omega_{31}$ ($\Delta_{c\pm}=\omega_{c\pm}-\omega_{32}$) is taken to be the probe (coupling) detunings from transition $|1\rangle \leftrightarrow |3\rangle$ ($|2\rangle \leftrightarrow |3\rangle$), while $\Delta_b=\omega_{c-}-\omega_{c+}=\omega_{p-}-\omega_{p+}$ is set as the bichromatic detuning between the BW and the FW coupling (probe) photons.

The coupling field is supposed to be slowly modulated in time, and the probe field to be a pulse with a slowly varying envelope. Since in a realistic atomic level configuration, $k_{p_\pm}\simeq k_{c_\pm}$,[2] in Eqs. (4) we choose the wave vectors of the coupling field components as the *central* wave vectors for the probe pulse components as well.[3]

We adopt in the following a semiclassical result [47,49] for a single-mode driving field where evolutions of the atomic variables are described in terms of an ensemble-averaged form of the density-matrix equations of motion [21,22]. The relevant Liouville equation for a group of atoms moving at velocity υ in the $+z$ direction may be written in this case as

$$i\hbar\left(\frac{\partial}{\partial t}+\upsilon\frac{\partial}{\partial z}\right)\rho = [H_I,\rho]+R\rho, \tag{5}$$

where R describes relaxation processes due, for example, to spontaneous emission and atomic collisions. The specific dynamics of the spin and optical coherences for the three-level EIT system shown in Fig. 1 are derived from Eq. (5) as

$$\begin{aligned}(\partial_t+\upsilon\partial_z)\rho_{21} &= -\gamma_{21}\rho_{21}+i\Omega_c^*\rho_{31},\\ (\partial_t+\upsilon\partial_z)\rho_{31} &= -\gamma_{31}\rho_{31}+i\Omega_c\rho_{21}+i\Omega_p,\end{aligned} \tag{6}$$

where γ_{21} and γ_{31} denote the spin and optical coherences dephasing rates, respectively. In deriving Eqs. (6), we have

[2] A typical hyperfine splitting (ω_{21}) for ^{87}Rb atoms is of the order 6.8 GHz, which amounts to a fairly small mismatch, $\Delta k\sim 0.14\ \text{mm}^{-1}$, between $k_{p_\pm}$ and $k_{c_\pm}$.

[3] In our case, as described by Eqs. (4), the coupling field of Eq. (1) becomes $E_c=E_{c+}(t)e^{-i\omega_{c+}t+ik_{c+}z}+E_{c-}(t)e^{-i\omega_{c-}t-ik_{c-}z}$ [with $\Omega_{c\pm}(t)=E_{c\pm}(t)d_{32}/2\hbar$], and the probe field of Eq. (2) becomes $E_p=\epsilon_{p+}(z,t)e^{-i\omega_{p+}t+ik_{c+}z}+\epsilon_{p-}(z,t)e^{-i\omega_{p-}t-ik_{c-}z}$ [with $\Omega_{p\pm}(z,t)=\epsilon_{p\pm}(z,t)d_{31}/2\hbar$].

assumed that the two probe components $E_{p_\pm}$ are weak enough so that $\rho_{11} \simeq 1$ and $\rho_{22} \simeq \rho_{33} \simeq \rho_{32} \simeq 0$.

The spin coherence in Eqs. (6) is then expanded into spatial Fourier components as

$$\rho_{21}(z,t,\upsilon) = e^{-i(\Delta_{p+}-\Delta_{c+})t} \times \sum_{n=-\infty}^{+\infty} \rho_{21}^{(2n)}(z,t,\upsilon) e^{+in(k_{c+}+k_{c-})z+in\Delta_b t}, \quad (7)$$

and likewise for the optical coherence,

$$\rho_{31}(z,t,\upsilon) = e^{-i\Delta_{p+}t+ik_{c+}z} \sum_{n=0}^{+\infty} \rho_{31}^{(2n+1)}(z,t,\upsilon) \times e^{+in(k_{c+}+k_{c-})z+in\Delta_b t} + e^{-i(\Delta_{p+}+\Delta_b)t-ik_{c-}z} \times \sum_{n=0}^{-\infty} \rho_{31}^{(2n-1)}(z,t,\upsilon) e^{+in(k_{c+}+k_{c-})z+in\Delta_b t}. \quad (8)$$

Inserting Eqs. (4), (7), and (8) into Eqs. (6), we arrive at an infinite set of mutually coupled equations,[4]

$$\begin{aligned} \partial_t \rho_{21}^{(2n)} &= -\gamma_{21}^{(2n)} \rho_{21}^{(2n)} + i\Omega_{c+}\rho_{31}^{(2n+1)} + i\Omega_{c-}\rho_{31}^{(2n-1)} \\ \partial_t \rho_{31}^{(2n+1)} &= -\gamma_{31}^{(2n+1)} \rho_{31}^{(2n+1)} + i\Omega_{c+}\rho_{21}^{(2n)} \\ &\quad + i\Omega_{c-}\rho_{21}^{(2n+2)} + i\Omega_{p+}\delta_{n,0}, \end{aligned} \quad (9)$$

with $\gamma_{31}^{(2n+1)} = \gamma_{31} - i\Delta_{p+} + in\Delta_b + i\upsilon(n+1)k_{c+} + i\upsilon n k_{c-}$ for $n \geqslant 0$, and

$$\begin{aligned} \partial_t \rho_{21}^{(2n)} &= -\gamma_{21}^{(2n)} \rho_{21}^{(2n)} + i\Omega_{c+}\rho_{31}^{(2n+1)} + i\Omega_{c-}\rho_{31}^{(2n-1)} \\ \partial_t \rho_{31}^{(2n-1)} &= -\gamma_{31}^{(2n-1)} \rho_{31}^{(2n-1)} + i\Omega_{c+}\rho_{21}^{(2n-2)} \\ &\quad + i\Omega_{c-}\rho_{21}^{(2n)} + i\Omega_{p-}\delta_{n,0}, \end{aligned} \quad (10)$$

with $\gamma_{31}^{(2n-1)} = \gamma_{31} - i\Delta_{p+} + i(n-1)\Delta_b + i\upsilon n k_{c+} + i\upsilon(n-1)k_{c-}$ for $n \leqslant 0$. In addition, one has the same value, $\gamma_{21}^{(2n)} = \gamma_{21} - i(\Delta_{p+} - \Delta_{c+}) + in\Delta_b + i\upsilon n(k_{c+} + k_{c-})$, of the spin dephasing rate for both $n \geqslant 0$ and $n \leqslant 0$. All dependencies of spin and optical coherence terms have been omitted in Eqs. (9) and (10).

The coupled Liouville Eqs. (9) and (10), if truncated at a suitable $|n|$, may be numerically solved to generate $\rho_{31}^{(\pm 1)}(z,t,\upsilon)$. This in turn is to be averaged over all possible velocities along the z direction of a typical Maxwell distribution $N(\upsilon) = \frac{N_0}{\upsilon_d\sqrt{\pi}} e^{-\upsilon^2/\upsilon_d^2}$ for a thermal atomic sample at a temperature T; that is,

$$\rho_{31}^{(\pm 1)}(z,t) = \int_{-\infty}^{+\infty} \rho_{31}^{(\pm 1)}(z,t,\upsilon) N(\upsilon)\, d\upsilon, \quad (11)$$

where the temperature T is directly related to the most probable speed $\upsilon_d = \sqrt{2KT/m}$ and hence to the probe transition residual Doppler width $\Delta_d \equiv \omega_{31}\upsilon_d/c$.

The probe dynamics in a SW driving configuration that mutually couples the FW and BW probe components is assessed by solving Maxwell's equations together with Eqs. (9) and (10) [39]. The relevant wave equations, in the slowly varying envelope approximation[5] for both probe and optical polarization fields, turn out to be

$$\begin{aligned} \partial_z \Omega_{p+} &= -\partial_t \Omega_{p+}/c + i\Delta k \Omega_{p+} + i\frac{\gamma_{31}\alpha_+}{2}\rho_{31}^{(+1)}, \\ \partial_z \Omega_{p-} &= +\partial_t \Omega_{p-}/c - i\Delta k \Omega_{p-} - i\frac{\gamma_{31}\alpha_-}{2}\rho_{31}^{(-1)}, \end{aligned} \quad (12)$$

with $\alpha_\pm = \frac{N_0 d_{31}^2}{\varepsilon_0 \hbar}\frac{k_{p\pm}}{\gamma_{31}}$ and $\Delta k = k_{p_\pm} - k_{c\pm}$.[6]

Equations (9)–(12) are our main result and apply in a rather general fashion when effects of light propagation in atomic samples driven into the SW-EIT configuration are to be investigated. It is, however, worthwhile mentioning two limiting cases here. For very cold atomic samples ($T = 0$) our theory can be seen to reduce to that used in Ref. [46], where the dynamics of a light pulse in SW dressed ultracold atoms has been studied. In this temperature range, Doppler effects are not important and the velocity averaging in Eq. (11) is likewise not relevant. In the opposite limit of warm atoms, the velocity averaging in Eq. (11) is most relevant and all higher-order coherence components are expected to be immaterial as in Ref. [30], where the light propagation dynamics is studied in SW dressed warm atoms. Since our Maxwell-Liouville Eqs. (9)–(12) are rather involved integrodifferential equations, analytical or asymptotic solutions are clearly hard to attain except for ultracold or warm atomic samples. This is possible when adiabatic and secular approximations as well as arbitrary initial-state assumptions [30,31] are made, which may, however, result in a significant underestimate of SLP decay [46].

In the next section we set $\Delta_{p+} = \Delta_{c+} = -\Delta_b/2$. For cold ^{87}Rb atoms at temperatures below 10 mK, we have $\upsilon/c < 10^{-8}$ and thus $n\upsilon\Delta_b/c < 0.1$ Hz for $n \leqslant 5$ and $\Delta_b = 3.0$ MHz [cf. Fig. 2(f)], so we may further assume that $k_{c-} = k_{c+}$ and $k_{p-} = k_{p+}$ in $\gamma_{21}^{(2n)}$ and $\gamma_{31}^{(2n\pm 1)}$. In this case, if we define $\Delta = \upsilon k_{c+} = \omega_{c+}\upsilon/c$ as the Doppler shift, the complex dephasing rates in Eqs. (9) and (10) simplify to

$$\begin{aligned} \gamma_{21}^{(2n)} &= \gamma_{21} + i2n(\Delta + \Delta_b/2), \\ \gamma_{31}^{(2n\pm 1)} &= \gamma_{31} + i(2n \pm 1)(\Delta + \Delta_b/2). \end{aligned} \quad (13)$$

It is clear that both transverse relaxations (γ_{21} and γ_{31}) and frequency detunings (Δ and Δ_b) affect the decay of higher-order coherence terms in Eqs. (9) and (10). Increasing values of Δ and Δ_b will produce a decrease in amplitudes of these higher-order coherence terms, and hence when only the Doppler shift is present, for instance, spin $[\rho_{21}^{(2n)}]$ and optical $[\rho_{31}^{(2n\pm 1)}]$ coherences decrease in inverse proportion to values

[4]The velocity-dependent terms $\upsilon\partial_z\rho_{31}^{(2n\pm 1)}$ on the left-hand side of Eqs. (9) and (10) have been purposely omitted, as the Fourier components $\rho_{31}^{(2n\pm 1)}$ vary slowly over spatial scales of the order of υ divided by the characteristic frequency of the time evolution of $\rho_{31}^{(2n\pm 1)}$, i.e., $\upsilon\partial_z\rho_{31}^{(2n\pm 1)} \ll \partial_t\rho_{31}^{(2n\pm 1)}$, and similarly for the Fourier spin terms $\upsilon\partial_z\rho_{21}^{(2n)} \ll \partial_t\rho_{21}^{(2n)}$.

[5]Both probe field and polarization amplitudes in Eqs. (12), proportional to $\Omega_{p_\pm}(z,t)$ and to $\rho_{31}^{\pm 1}(z,t)$, respectively, are assumed to vary slowly on time scales of an optical period. The probe field is further assumed to vary slowly on spatial scales of an optical wavelength ($\partial_z E_{p_\pm} \ll k_{p_\pm} E_{p_\pm}$).

[6]The small mismatch Δ_k (see footnote 2) arises from the fact that we work in the limit of $k_{p_\pm} \simeq k_{c_\pm}$ [cf. Eqs. (4)].

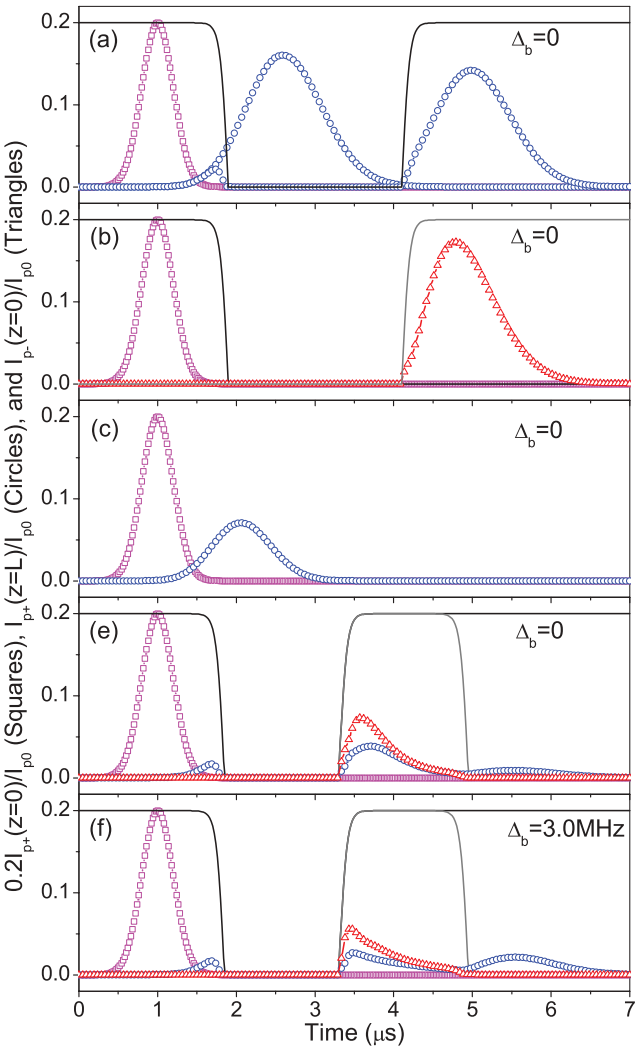

FIG. 2. (Color online) Transmission [(blue) circles] and reflection [(red) triangles] profiles of a probe pulse [(magenta) squares] incident on a sample of *cold* ^{87}Rb atoms driven by an SW coupling with time-modulated FW (black) and BW (gray) components. Numerical simulations correspond to the experimental data in Figs. 4(a–c), 4(e), and 4(f) of Ref. [32], whose labeling is maintained here for the sake of comparison. (a) The first probe transmission signal is obtained with $\Omega_{c+} \equiv 2.05$ MHz, while the second signal corresponds to storage and retrieval obtained with $\Omega_{c+} = 2.05$ MHz switched, first, off at $t_1 = 1.90$ μs and, then, on at $t_2 = 4.10$ μs. (b) Probe pulse storage by switching $\Omega_{c+} = 2.05$ MHz off at $t_1 = 1.90$ μs and then retrieval in the opposite direction by switching on $\Omega_{c-} = 2.05$ MHz at $t_2 = 4.10$ μs. (c) FW probe component transmission in the presence of $\Omega_{c-} \equiv 2.42$ MHz. (e, f) The FW coupling component $\Omega_{c+} = 2.05$ MHz is switched off at $t_1 = 1.85$ μs and then on at $t_2 = 3.30$ μs, while the BW coupling component $\Omega_{c-} = 2.05$ MHz is switched on at $t_2 = 3.30$ μs and off at $t_3 = 4.95$ μs, allowing for probe storage between t_1 and t_2 and SLP formation between t_2 and t_3. Equations (8) and (9) are truncated at $|n| = 3$ in (e), where $\Delta_b = 0$, but at $|n| = 1$ in (f), where $\Delta_b = 3.0$ MHz, to ensure convergence in each case. Other common parameters are $\Delta_d = 305$ kHz, corresponding to a temperature of 296 μK, $\Delta_{p+} = \Delta_{c+} = -\Delta_b/2$, $\gamma_{21} = 4.0$ kHz, $\gamma_{31} = 3.0$ MHz, $N_0 = 3.02 \times 10^{10}$ cm^{-3}, $L = 10$ mm, $d_{31} = 1.465 \times 10^{-29}$ C·m, $\lambda_{p+} = 780.792$ nm, and $\lambda_{c+} = 780.778$ nm. The incident probe pulse is assumed to have a Gaussian profile $I_p = I_{p0} \exp[-(t - t_0)^2/\tau^2]$, with $t_0 = 1.0$ μs and duration $\tau = 0.4$ μs.

of the product $n\upsilon \sim n\sqrt{T}$. At sufficiently high temperatures, only the zero-order term $\rho_{21}^{(0)}$ will then survive decay, whereas other higher-order terms [$\rho_{31}^{(\pm1,\pm3,\ldots)}$ and $\rho_{21}^{(\pm2,\pm4,\ldots)}$] may instead survive for temperatures approaching 0. It is then clear that, under the two-photon resonance condition ($\Delta_{p\pm} = \Delta_{c\pm}$) required to achieve EIT, the zero-order spin coherence $\rho_{21}^{(0)}$ always contributes to the SLP dynamics. Conversely, other higher-order spin coherences $\rho_{21}^{(\pm2,\pm4,\ldots)}$, whose nonzero frequency detunings grow with their orders, may quickly exceed the EIT window and become irrelevant to the SLP dynamics.[7] Just as the Doppler shift Δ experienced by thermal atoms restrains the development of higher-order coherence terms, a bichromatic detuning Δ_b may likewise be used to avoid losses in the process of SLP formation in cold atoms.

III. STATIONARY LIGHT GENERATION IN COLD THERMAL ATOMS

In this section, we use the theoretical approach developed in the previous section to investigate the SLP generation in a cold thermal atomic sample where the residual Doppler broadening is not negligible. In particular, we present numerical simulation, with an excellent agreement, for the experimental results as recently observed in such a low but finite temperature regime [32].

Using Eqs. (9)–(12), we simulate a set of experimental data shown in Fig. 4 of Ref. [32]. There, the FW signals (transmitted to the sample exit) and the BW signals (reflected to the sample entrance) of an incident probe pulse are reported for different experimental configurations and achieved by using different time modulations of the TW or SW coupling fields. Our predictions are shown in Fig. 2 and reproduce very well the corresponding plots in Fig. 4 of Ref. [32]. In particular, the atomic temperature is determined by simulating the data in Fig. 4(c) of Ref. [32], where the FW probe and the BW coupling are not in the Doppler-free configuration. Our best fit is obtained for $\Delta_d \simeq 305$ kHz, corresponding to an atomic temperature $T \simeq 296$ μK, which clearly amounts to a non-negligible Doppler effect. A further assessment of the relevance of Doppler broadening is made by again simulating the FW probe signals shown in Figs. 4(c) and 4(e) of Ref. [32] but using different values of Δ_d. This is done in Figs. 3(a) and 3(b), where a moderate change of the Doppler width Δ_d : 457 $\leftarrow$ 305 $\rightarrow$ 205 kHz (T : 665 $\leftarrow$ 296 $\rightarrow$ 134 μK) results in a significant departure of the theoretical curves from the experimental data. This makes clear that the proper inclusion of the residual Doppler broadening is essential to explain well experiments with cold thermal atoms, making approaches that work strictly at $T = 0$ somewhat unfit. We further note that the curves for $\Delta_d = 0$ and those for $\Delta_d = 61$ kHz are not far

[7]The overall decay of spin coherence ρ_{21} in Eq. (7) may also be envisaged to occur when Bloch vectors with different detunings gradually become out of phase with each other. Coherence components $\rho_{21}^{(2n)}$ in Eq. (7) decaying at different rates $\gamma_{21}^{(2n)}$ may in fact be associated with Bloch vectors precessing around different orientations [17] that depend directly on imaginary parts of complex rates $\gamma_{21}^{(2n)}$ in Eqs. (13). A similar description may be brought forward for the decay of coherence components $\rho_{31}^{(2n\pm1)}$ in Eq. (8).

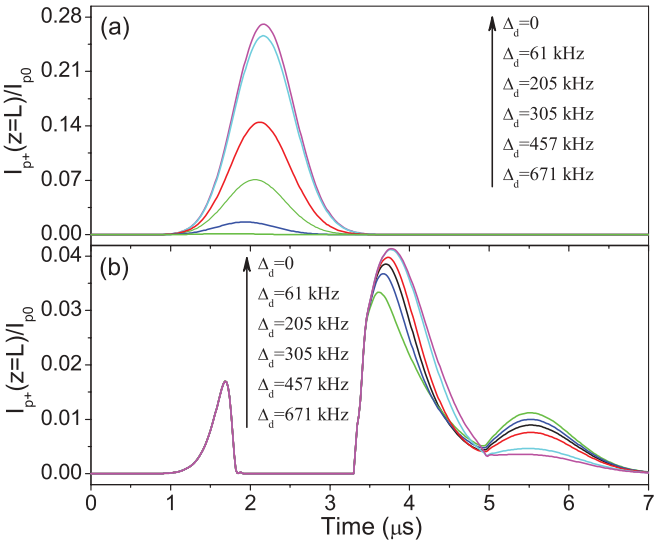

FIG. 3. (Color online) Transmitted probe signals as in Figs. 2(c) and 2(e) for different Doppler widths: $\Delta_d = 671$ kHz (green), 457 kHz (blue), 305 kHz (black), 205 kHz (red), 61 kHz (cyan), and 0 (magenta), from bottom to top, associated with a temperature of $T = 1.43$ mK, 665 μK, 296 μK, 134 μK, 11.9 μK, and 0, respectively. Equations (9) and (10) are truncated at $|n| = 1$ for $\Delta_d = 671$ kHz, $|n| = 2$ for $\Delta_d = 457$ kHz, $|n| = 3$ for $\Delta_d = 305$ kHz and $\Delta_d = 205$ kHz, $|n| = 4$ for $\Delta_d = 61$ kHz, and $|n| = 5$ for $\Delta_d = 0$, respectively, to ensure convergence in each case.

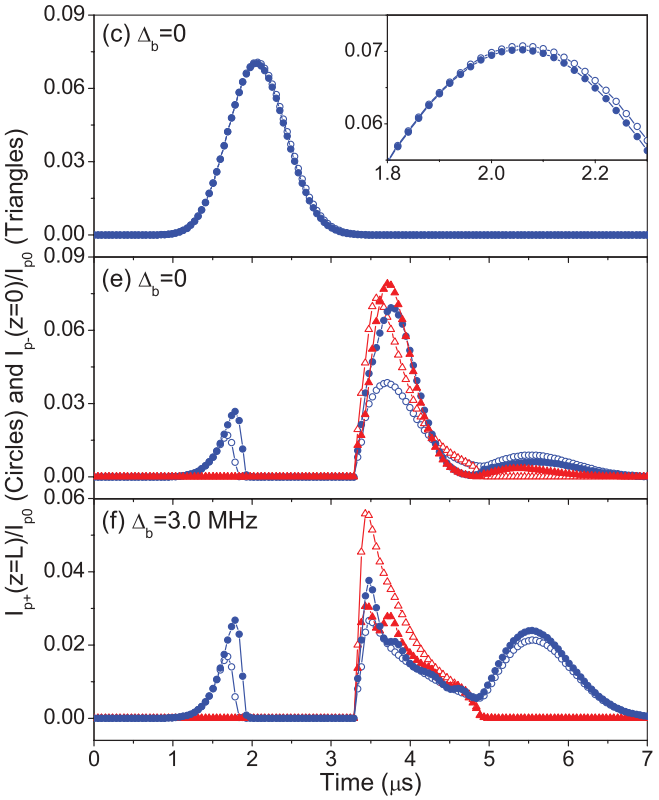

FIG. 4. (Color online) Transmitted (circles) and reflected (triangles) probe signals as in Figs. 2(c), 2(e), and 2(f). Curves with filled symbols were obtained by adopting the method in Ref. [32] with $\gamma_{21} = 4.0$ kHz for $\rho_{21}^{(0)}$ but $\gamma_{21} = 102$ kHz for $\rho_{21}^{(\pm 2)}$. Curves with open symbols, however, were obtained with our approach.

separated, meaning that the residual Doppler broadening may safely be neglected when $T \lesssim 10$ μK.

It is worth noting here that the preceding experiment has been simulated in Ref. [32] with a different set of Maxwell-Liouville equations. In fact, a set of lower-order truncated equations was used there, retaining only the $\rho_{21}^{(0)}$, $\rho_{31}^{(\pm 1)}$, and $\rho_{21}^{(\pm 2)}$ terms and adopting a very high dephasing rate for $\rho_{21}^{(\pm 2)}$. This is an ingenious *ad hoc* procedure to mimic the effect of Doppler broadening, which reproduces roughly the observed data except for some of the fine details, for which, however, a better fit is provided by our Eqs. (9)–(12). In Fig. 4(e) of Ref. [32], the numerically calculated FW signal in fact deviates from the experimentally observed FW signal for times between 3 and 5 μs and has an unexpected dip centered at 4.7 μs. In Fig. 4(f) of Ref. [32], a few puzzling oscillations are also found for the theoretical curves of both FW and BW signals between 3 and 5 μs. At variance with this, as shown in Fig. 4 for comparison, our approach does not show such discrepancies in the fine details of the experimental data.

A very important issue concerns the order at which the Liouville Eqs. (9) and (10) should be truncated to ensure numerical convergence. In Fig. 5 we plot the FW and BW probe signals with different cutoff values of $|n|$. As we can see, the curves for $|n| = 2$ and those for $|n| = 3$ are almost indistinguishable, so we may conclude that the truncation at $|n| = 3$ used in Fig. 2(e) is appropriate, while a lower-order truncation would introduce significant errors. When only the sample temperature is relevant, the appropriate cutoff value simply decreases with the increasing temperature as the Doppler broadening significantly suppresses the coupling to higher-order coherence components. Within our approach, this is apparent from the dependence of the complex dephasing rates $\gamma_{21}^{(2n)}$ and $\gamma_{31}^{(2n\pm 1)}$ on the product $n \times \Delta$, as discussed after Eqs. (13). From the various cutoff values used to

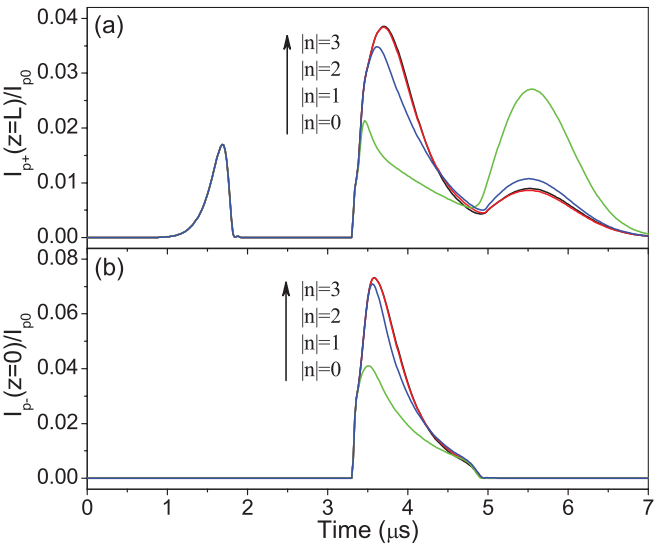

FIG. 5. (Color online) Transmitted (a) and reflected (b) probe signals as in Fig. 2(e) for different cutoff values of $|n|$ with $\Delta_d = 305$ kHz and $\Delta_b = 0$. Green, blue, red, and black curves correspond, from bottom to top, to $|n| = 0$, 1, 2, and 3, respectively.

ensure numerical convergence in Fig. 3, it is clear that such temperature effects are very effective in limiting the coupling to higher-order coherence components.

On the contrary, in Fig. 2(f) we have truncated the Liouville Eqs. (9) and (10) at $|n| = 1$ [i.e., retaining $\rho_{21}^{(0)}$, $\rho_{31}^{(\pm 1)}$, $\rho_{21}^{(\pm 2)}$, and $\rho_{31}^{(\pm 3)}$] due to the large bichromatic detuning, $\Delta_b = 3.0$ MHz, employed in this case. The suitability of such a truncation has also been numerically checked as above. In this case, our results confirm the validity of the proposal put forth in Ref. [32] to take advantage of a large bichromatic detuning to suppress the excitation of higher-order coherences and improve the formation of an SLP. As a matter of fact, the efficient coupling to higher-order coherences, which takes place when no bichromatic detuning is employed and at extremely low temperatures where the Doppler broadening is immaterial, is a very significant mechanism of loss and diffusion that severely affect SLPs as we have recently discussed [46].

To the best of our knowledge, the theoretical approach presented here is the only one available to cover the limits both of negligible and of significant Doppler broadening on equal footing, without invoking additional approximations or *ad hoc* assumptions. Finally, it is to be emphasized that the suitable cutoff value of $|n|$ to be used in actual numerical simulations depends critically on the Doppler broadening width Δ_d (i.e., the sample temperature T) and on the bichromatic detuning Δ_b, as discussed previously, but it also depends in general on the sample optical depth as well as on the SW coupling Rabi frequencies.[8]

IV. CONCLUSIONS

In summary, we have established a rather general approach to numerically examine the propagation dynamics of a weak light pulse inside atomic samples where it is essential to take the Doppler broadening into account. The atomic samples are assumed to be dressed by an SW coupling field with two counter-propagating components so that the spin and optical coherences consist of a series of Fourier components excited by the successive Bragg scattering of FW and BW photons. Because these coherence components decrease in amplitude with their increasing orders, we are allowed to truncate the Fourier-expanded Maxwell-Liouville equations at a suitable integer without introducing appreciable errors.

A quite satisfactory check of our numerical results has been carried out through a comparison with a recent experiment on SLPs in cold thermal ^{87}Rb atoms [32], whose formation entails the presence of higher-order spin and optical coherence terms even for atomic temperatures in the millikelvin range. Neglecting the residual Doppler broadening or discarding the higher-order coherence terms will lead to appreciable errors in the theoretical curves relevant to the experimental data. A large bichromatic detuning, however, allows us to truncate the Maxwell-Liouville equations at a much lower integer yet without introducing notable errors. This is because the higher-order coherence terms are prevented from excitation in the presence of a large bichromatic detuning.

We expect that this general approach may be further extended to devise new schemes for lossless SLPs generation and interaction, for example, in solid materials doped with impurities such as Pr^{3+}:Y_2SiO_5 and diamond containing N-V color centers [50,51], where inhomogeneous broadening plays an important role.

[8]For instance, the Fourier-expanded Liouville equations are truncated at $|n| = 30$ in Refs. [39], [40], and [46] because there the ultracold ($T = 0$) atomic sample is much denser ($N \sim 1.0 \times 10^{13}$ cm^{-3}) and the SW coupling is much stronger ($\Omega_{c+} \sim \Omega_{c-} \sim 25$ MHz).

ACKNOWLEDGMENTS

Jin-Hui Wu gratefully acknowledges the hospitality of Scuola Normale Superiore in Pisa. Helpful discussions with Prof. Ite A. Yu on details of the experiment in Ref. [32] are gratefully acknowledged. This work was supported by Grant Nos. NSFC-10874057 and NBRP-2006CB921103 (China) and by the CRUI-British Council Partnership Program on "Atoms and Nanostructures," Azione Integrata Grant No. IT09L244H5 from MIUR, PRIN Grant No. 2006-021037 from MIUR, and CNR Italy Contract No. 0008233.

[1] J. I. Cirac, P. Zoller, H. J. Kimble, and H. Mabuchi, Phys. Rev. Lett. **78**, 3221 (1997).
[2] A. Kuzmich, W. P. Bowen, A. D. Boozer, A. Boca, C. W. Chou, L.-M. Duan, and H. J. Kimble, Nature (London) **423**, 731 (2003).
[3] C. H. van der Wal, M. D. Eisaman, A. Andre, R. L. Walsworth, D. F. Phillips, A. S. Ziborv, and M. D. Lukin, Science **301**, 196 (2003).
[4] M. D. Lukin and A. Imamoglu, Nature (London) **413**, 273 (2001).
[5] H. Mabuchi and A. C. Doherty, Science **298**, 1372 (2002).
[6] M. Fleischhauer and M. D. Lukin, Phys. Rev. Lett. **84**, 5094 (2000).
[7] C. Liu, Z. Dutton, C. H. Behroozi, and L. V. Hau, Nature (London) **409**, 490 (2001).
[8] T. Chaneliere, D. N. Matsukevich, S. D. Jenkins, S.-Y. Lan, T. A. B. Kennedy, and A. Kuzmich, Nature (London) **438**, 833 (2005).
[9] K. S. Choi, H. Deng, J. Laurat, and H. J. Kimble, Nature (London) **452**, 67 (2008).
[10] K. Bergmann, H. Theuer, and B. W. Shore, Rev. Mod. Phys. **70**, 1003 (1998).
[11] C. Y. Ye, V. A. Sautenkov, Y. V. Rostovtsev, and M. O. Scully, Opt. Lett. **28**, 2213 (2003).
[12] L. Wang, X.-L. Song, A.-J. Li, H.-H. Wang, X.-G. Wei, Z.-H. Kang, Y. Jiang, and J.-Y. Gao, Opt. Lett. **33**, 2380 (2008).
[13] D. A. Braje, V. Balic, G. Y. Yin, and S. E. Harris, Phys. Rev. A **68**, 041801(R) (2003).
[14] H. Kang, G. Hernandez, and Y. Zhu, Phys. Rev. Lett. **93**, 073601 (2004).
[15] Y. P. Zhang, A. W. Brown, and M. Xiao, Phys. Rev. Lett. **99**, 123603 (2007).
[16] S. Li, X. Yang, X. Cao, C. Zhang, C. Xie, and H. Wang, Phys. Rev. Lett. **101**, 073602 (2008).

[17] M. O. Scully and M. S. Zubairy, *Quantum Optics* (Cambridge University Press, Cambridge, UK, 1997), Chap. 7, pp. 220–247.
[18] A. B. Matsko, O. Kocharovskaya, Y. V. Rostovtsev, G. R. Welch, A. S. Zibrov, and M. O. Scully, Adv. At. Mol. Opt. Phys. **46**, 191 (2001).
[19] M. Fleischhauer, A. Imamoglu, and J. P. Marangos, Rev. Mod. Phys. **77**, 633 (2005).
[20] H. Y. Ling, Y. Q. Li, and M. Xiao, Phys. Rev. A **57**, 1338 (1998).
[21] F. Silva, J. Mompart, V. Ahufinger, and R. Corbalan, Europhys. Lett. **51**, 286 (2000).
[22] F. Silva, J. Mompart, V. Ahufinger, and R. Corbalan, Phys. Rev. A **64**, 033802 (2001).
[23] D. V. Strekalov, A. B. Matsko, and N. Yu, Phys. Rev. A **76**, 053828 (2007).
[24] I.-H. Bae, H. S. Moon, M.-K. Kim, L. Lee, and J. B. Kim, Opt. Express **18**, 1389 (2010).
[25] A. Andre and M. D. Lukin, Phys. Rev. Lett. **89**, 143602 (2002).
[26] X. M. Su and B. S. Ham, Phys. Rev. A **71**, 013821 (2005).
[27] M. Artoni and G. C. La Rocca, Phys. Rev. Lett. **96**, 073905 (2006).
[28] D. Petrosyan, Phys. Rev. A **76**, 053823 (2007).
[29] M. Bajcsy, A. S. Zibrov, and M. D. Lukin, Nature (London) **426**, 638 (2003).
[30] F. E. Zimmer, A. Andre, M. D. Lukin, and M. Fleischhauer, Opt. Commun. **264**, 441 (2006).
[31] K. R. Hansen and K. Mølmer, Phys. Rev. A **75**, 053802 (2007); **75**, 065804 (2007).
[32] Y.-W. Lin, W.-T. Liao, T. Peters, H.-C. Chou, J.-S. Wang, H.-W. Cho, P.-C. Kuan, and I. A. Yu, Phys. Rev. Lett. **102**, 213601 (2009).
[33] G. Nikoghosyan and M. Fleischhauer, Phys. Rev. A **80**, 013818 (2009).
[34] J. Otterbach, R. G. Unanyan, and M. Fleischhauer, Phys. Rev. Lett. **102**, 063602 (2009).
[35] J. Otterbach, J. Ruseckas, R. G. Unanyan, G. Juzeliunas, and M. Fleischhauer, Phys. Rev. Lett. **104**, 033903 (2010).
[36] T. Peters, Y.-H. Chen, J.-S. Wang, Y.-W. Lin, and I. A. Yu, Opt. Lett. **35**, 151 (2010).
[37] A. W. Brown and M. Xiao, Opt. Lett. **30**, 699 (2005).
[38] J. Wang, C. Hang, and G. X. Huang, Phys. Lett. A **366**, 528 (2007).
[39] J.-H. Wu, M. Artoni, and G. C. La Rocca, J. Opt. Soc. Am. B **25**, 1840 (2008).
[40] J.-H. Wu, M. Artoni, and G. C. La Rocca, Phys. Rev. Lett. **103**, 133601 (2009).
[41] A. Andre, M. Bajcsy, A. S. Zibrov, and M. D. Lukin, Phys. Rev. Lett. **94**, 063902 (2005).
[42] S. A. Moiseev and B. S. Ham, Phys. Rev. A **71**, 053802 (2005).
[43] B. S. Ham, Appl. Phys. Lett. **88**, 121117 (2006).
[44] Y. Xue and B. S. Ham, Phys. Rev. A **78**, 053830 (2008).
[45] S. A. Moiseev and B. S. Ham, Phys. Rev. A **73**, 033812 (2006).
[46] J.-H. Wu, M. Artoni, and G. C. La Rocca, Phys. Rev. A **81**, 033822 (2010).
[47] V. S. Letokhov and V. P. Chebotayev, *Nonlinear Laser Spectroscopy, Springer Series in Optical Sciences, Vol. 4* (Springer-Verlag, Berlin, 1997).
[48] S.-Q. Kuang, R.-G. Wan, P. Du, Y. Jiang, and J.-Y. Gao, Opt. Express **16**, 15455 (2008).
[49] B. J. Feldman and M. S. Feld, Phys. Rev. A **1**, 1375 (1970).
[50] A. V. Turukhin, V. S. Sudarshanam, M. S. Shahriar, J. A. Musser, B. S. Ham, and P. R. Hemmer, Phys. Rev. Lett. **88**, 023602 (2001).
[51] J.-H. Wu, G. C. La Rocca, and M. Artoni, Phys. Rev. B **77**, 113106 (2008).